European Journal of Medicinal Chemistry 125 (2017) 1268–1278

Contents lists available at ScienceDirect

European Journal of Medicinal Chemistry

journal homepage: http://www.elsevier.com/locate/ejmech

Research paper

3-Aroylindoles display antitumor activity in vitro and in vivo: Effects of N1-substituents on biological activity

Hsueh-Yun Lee [a], Jiann-Fong Lee [a], Sunil Kumar [a], Yi-Wen Wu [b], Wei-Chun HuangFu [c], Mei-Jung Lai [d], Yu-Hsuan Li [a], Hsiang-Ling Huang [a], Fei-Chiao Kuo [a], Che-Jen Hsiao [e], Chun-Chun Cheng [c], Chia-Ron Yang [b, *], Jing-Ping Liou [a, **]

[a] School of Pharmacy, College of Pharmacy, Taipei Medical University, Taipei 11031, Taiwan
[b] School of Pharmacy, College of Medicine, National Taiwan University, Taipei, Taiwan
[c] The Ph.D. Program for Cancer Biology and Drug Discovery, College of Medical Science and Technology, Taipei Medical University, Taipei, Taiwan
[d] Center for Translational Medicine, Taipei Medical University, Taiwan
[e] Department of Pharmacology, College of Medicine, Taipei Medical University, Taiwan

ARTICLE INFO

Article history:
Received 16 July 2016
Received in revised form
24 October 2016
Accepted 14 November 2016
Available online 15 November 2016

Keywords:
Anticancer agents
Histone deacetylase inhibitors
3-Aroylindoles
Tubulin polymerization inhibition

ABSTRACT

A series of 3-aroylindole hydroxamic acids (**10**–**17**) were developed based on the concept of a structural combination of tubulin and histone deacetylase (HDAC) inhibitors. This was accomplished by introducing hydroxamic acid-containing moieties at the N1 position of the tubulin assembly inhibitor, compound **9** (SCB01A, BPR0L075, phase II trial). Most of synthetic compounds produced in this way displayed comparable HDAC inhibitory activity, and four (**10**, **12**–**14**) of them also inhibit tubulin assembly. Notably, compound **12** possesses not only tubulin and HDAC inhibitory activity but also shows HDAC6 selectivity over other HDAC isoforms. In addition, it exhibits remarkable inhibitory activity against the growth cancer cells in vitro and in vivo (PC3 and RPMI-8226 cells). Notably, it suppresses the growth of multiple myeloma xenografts without leading to the death of teated animals like reference compound. In sum, this study provided potential compounds with safer profiles for cancer treatment.

1. Introduction

To increase the structural diversity, the combination of specific motif from different classes of bioactive molecules has become a practical methodology in the field of medicinal chemistry. A literature survey indicated that histone deacetylase (HDAC) protein is commonly used to validate this strategy of structural combination, together with various biological targets. For example, Guerrant et al. have developed dual HDAC/Topo II inhibitors [1], and Lin et al. have synthesized a series of dual HDAC and HMG-coA reductase inhibitors [2]. Histone deacetylase (HDAC) is an attractive target, four HDAC inhibitors (SAHA [3], FK228 [4,5], PXD101 [6,7], and LBH589 [8,9]) having been approved by the US FDA for the treatment of cutaneous or refractory peripheral T-cell lymphoma or multiple myeloma. In addition, many HDAC inhibitors such as MS-275 (**6**) [10] are currently in clinical trials and our previously developed 1-arylsulfonyl-5-(*N*-hydroxyacrylamide)indoles (**7**) [11] and azaindolylsulfonamides (**8**) [12] also exhibit potent HDAC inhibitory activity and marked cytotoxicity. The potent antiproliferative activity of most HDAC inhibitors achieved by addressing epigenetic disorders can be attributed to the characteristic hydroxamic acid group [13,14]. The development of antitubulin agents has been intensively progressed for several decades, specifically in development of combretastatin analogous due to their evident structural requirements such as *Z*-geometrical conformation and 3,4,5-trimethoxyphenyl group [15]. Currently, research attention was shifted to the strategy of structural combination. For instance, Zhang et al. combined natural antitubulin agents or their analogous like colchicine and 4'-demethyl-4-deoxypodophyllotoxin with HDAC specific moieties such as hydroxamic acid and 2-aminobenzamide [16–18]. The strategy of structural combination may open a new avenue and attracts our attention to the utilization of our previously synthesized antitubulin agents.

The previous study on the modification of **9** (SCB01A, BPR0L075) revealed that the attachments such as furoyl, thiophenecarbonyl, and benzoyl at N1 position still retained its antiproliferative activity [19]. In addition, the presence of these groups cited above had no effect on the mechanism of action of related derivatives, which

* Corresponding author.
** Corresponding author.
E-mail addresses: cryang@ntu.edu.tw (C.-R. Yang), jpl@tmu.edu.tw (J.-P. Liou).

http://dx.doi.org/10.1016/j.ejmech.2016.11.033
0223-5234/

revealed the tolerance of structural modification at N1 position of compound **9**. In order to explore the effect of N1 substitutions on biological activity, we chose compound **9**, a potent antitubulin agent with concise structure and remarkable antiproliferative activity in vitro and in vivo currently in clinical trials (phase II), for a test of this precept [20,21]. A variety of hydroxamic acid-containing moieties presented in Fig. 1 (in blue) were selected from surveys of several potent HDAC inhibitors, which are expected to contribute HDAC inhibitory activity. According to an earlier SAR study, the N1 position of compound **9** can accommodate substitutions without significant influence on the antiproliferative activity. In an attempt to develop dual functional compounds, introduction of hydroxamic acid-containing moieties at the N1 position of compound **9** yielded a series of 3-aroylindole hydroxamic acids (**10**–**17**) and the structure-activity relationships (SAR), HDAC enzymatic assays, effects on tubulin assembly, and antitumor activity of the compounds in vivo were explored (see Fig. 2).

2. Results and discussion

2.1. Chemistry

Syntheses of compounds **10**, **11**, and **15** are shown in Scheme 1. Two 3-aroylindoles (**9** and **18**) were treated first with NaH and then with bromobenzensulfonyl chloride, yielding compounds **19**–**21**. The resulting compounds **19**–**21** were coupled with *tert*-butyl acrylate under the conditions of Heck olefination to give the corresponding cinnamates (**22**–**24**). The ester groups in **22**–**24** were hydrolyzed with TFA and the resulting products were allowed to react with NH_2OTHP in the presence of EDC·HCl and HOBt to yield the corresponding *O*-protected *N*-hydroxamides which were deprotected with 10% TFA to yield compounds **10**, **11**, and **15**.

Scheme 2 shows the synthesis of compounds **12**–**14** and **16**–**17**. 3-Aroyindoles (**9**, **18**, and **25**) was treated with NaH and then reacted with substituted benzyl halides to afford compounds **26**–**29**. The ester group of **26**–**27** was hydrolyzed with 1 N KOH to yield the corresponding carboxylic acids which were then subjected to amidation with NH_2OTHP and deprotection with 10% TFA, yielding the corresponding *N*-hydroxamic acids (**12**, **17**). Alternatively, the carboxylic acid obtained from compound **26** was reacted with *o*-phenylenediamine, the core structure of compound **6**, in the presence of EDC·HCl and HOBt to afford compound **14**. Compounds **28**–**29** underwent Heck olefination with *tert*-butyl acrylate and following the subsequent ester hydrolysis, amide formation with NH_2OTHP and TFA deprotection, afforded the corresponding *N*-hydroxamic acids (**13**, **16**).

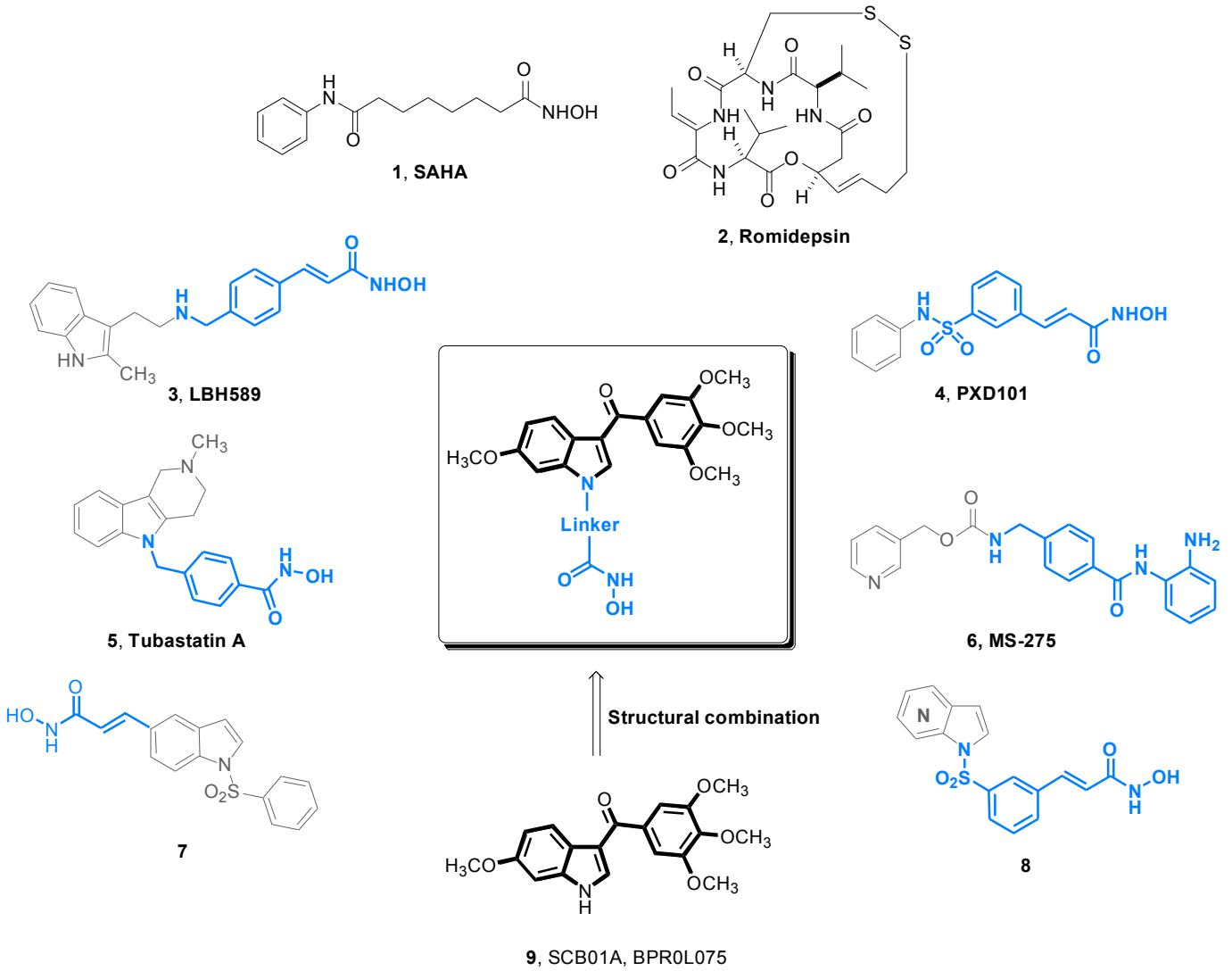

Fig. 1. The design of 3-aroylindole hydroxamic acids.

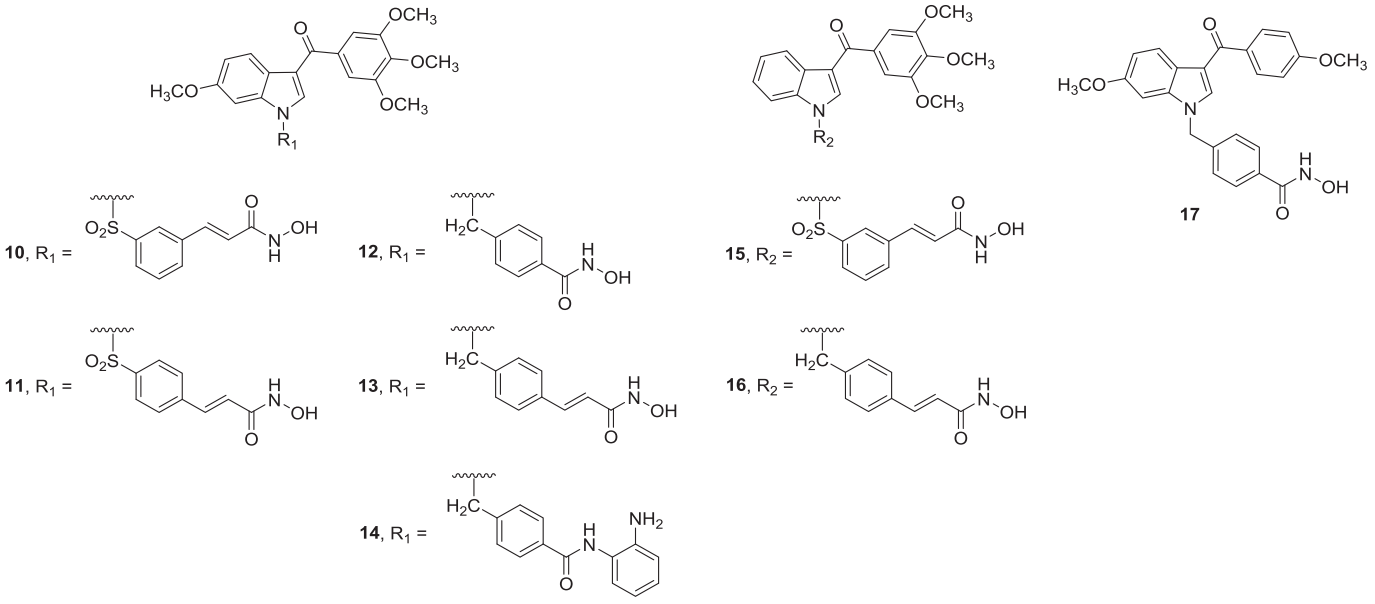

Fig. 2. Structures of designed compounds (**10**–**17**).

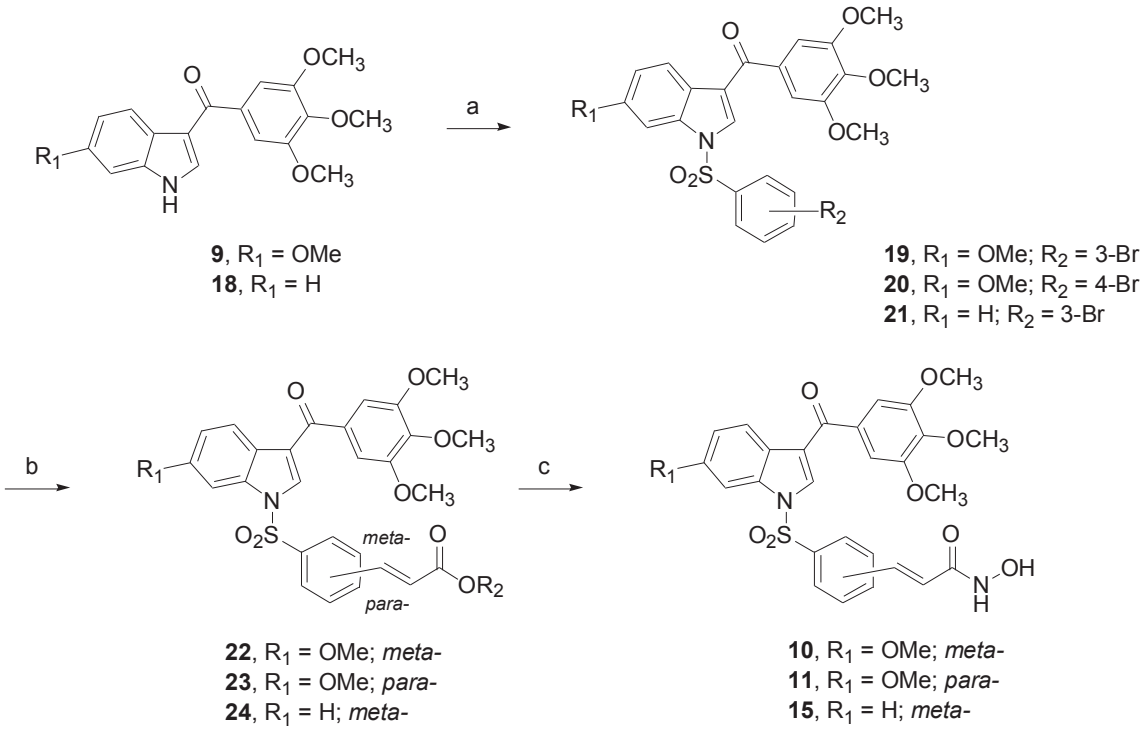

Scheme 1. Reagents and conditions: (a) NaH, bromobenzenesulfonyl chlorides, DMF, rt; (b) i. $Pd(OAc)_2$, PPh_3, NEt_3, K_2CO_3, *tert*-butyl acrylate, DMF, 100 °C; (c) i. CF_3COOH, rt; ii. EDC·HCl, HOBt, NH_2OTHP, NMM, DMF, rt; iii CF_3COOH/CH_3OH, rt.

2.2. Biological evaluation

2.2.1. HeLa nuclear HDAC enzyme inhibition

To determine if the introduction of a hydroxamic acid moiety confers anti-HDAC activity on this series of compounds, the inhibition of HeLa nuclear HDAC activity by the synthesized compounds was assessed (Table 1). The introduction of an *o*-aminobenzamide unit at the N-1 position (**14**) has a negligible influence on HDAC enzymatic activity. Compared with the effect of the *N*-hydroxylacrylamide moiety in **10** and **11**, this moiety can be seen to favor the meta position of the sulfonyl linker. However, this is not observed in compound **13** which has a methylene linker para to the *N*-hydroxylacrylamide moiety. Compounds **10**, **13**, and **17** exhibited comparable anti-HDAC activity in SAHA, whereas compounds **16** and **15** showed slightly weaker potency than that of the reference compound. These results indicate that the introduction of a hydroxamic acid-containing moiety at N1 of compound **9** contributes to the anti-HDAC activity of these compounds.

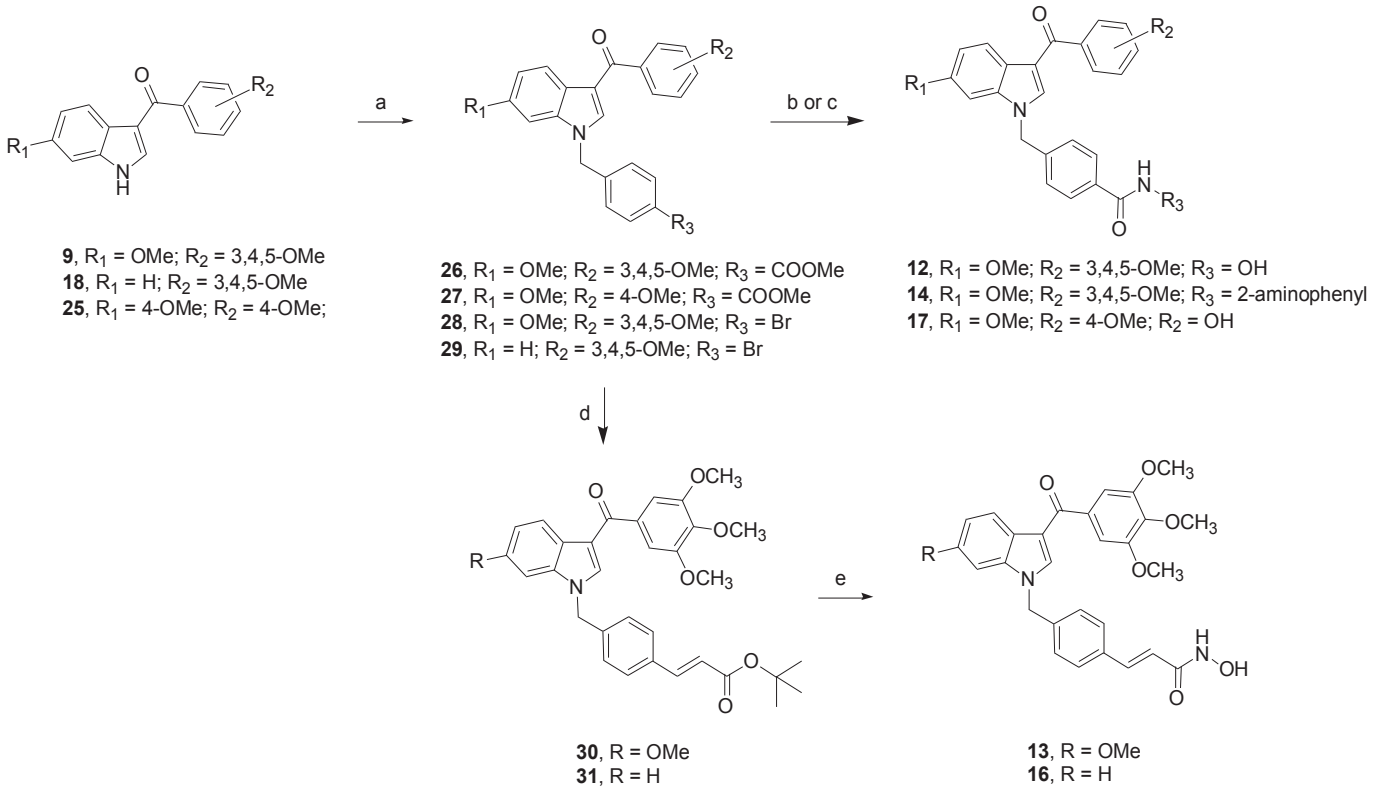

Scheme 2. Reagents and conditions: (a) NaH, 4-bomobenzyl bromide or methyl 4-(chloromethyl)benzoate, DMF, rt; (b) i. 1 N LiOH, MeOH, reflux; ii. EDC·HCl, HOBt, NH_2OTHP, NMM, DMF, rt; iii CF_3COOH/CH_3OH, rt. (c) For **26**: i. 1 N LiOH, MeOH, reflux; ii. *o*-phenylenediamine, HOBt, EDC·HCl, NMM, DMF; (d) For **28** and **29**: i. $Pd(OAc)_2$, PPh_3, NEt_3, K_2CO_3, *tert*-butyl acrylate, DMF, 100 °C; (e) i. CF_3COOH, rt; ii. EDC·HCl, HOBt, NH_2OTHP, NMM, DMF, rt; iii CF_3COOH/CH_3OH, rt.

Table 1
HDAC Inhibitory Activity (IC_{50}) and Antiproliferative activity of Compounds **1**, **9** and **10**–**17**.

	HeLa nuclear HDACs IC_{50} (nM)	$IC_{50} \pm SD$[a] (nM)		
Compd		A549	HCT116	PC3
10	135.45 ± 4.23	72.52 ± 5.22	43.91 ± 0.81	33.09 ± 0.97
11	>10,000	119.56 ± 7.15	70.34 ± 1.71	66.74 ± 0.89
12	610.81 ± 5.32	205.68 ± 3.38	484.57 ± 3.94	179.26 ± 6.42
13	146.66 ± 7.46	677.67 ± 7.04	1674.60 ± 68.13	665.57 ± 23.67
14	>10,000	208.38 ± 5.41	231.38 ± 4.53	156.93 ± 5.45
15	172.22 ± 8.22	4592.88 ± 190.67	6684.85 ± 50.68	5774.80 ± 299.39
16	177.55 ± 13.61	1898.46 ± 96.21	5498.10 ± 137.73	2601.66 ± 131.43
17	144.69 ± 4.62	939.90 ± 34.26	1896.28 ± 19.16	1841.38 ± 50.50
1	120.06 ± 5.55	476.86 ± 20.09	1488.60 ± 59.48	873.26 ± 50.85
9[b]	–	23 ± 6	–	–

[a] SD: standard deviation, all experiments were independently performed at least three times.
[b] Data from ref. [20].

2.2.2. *In vitro cell growth inhibition*

The antiproliferative activities of the synthetic 3-aroylindole hydroxamic acids (**10**–**17**), and the reference compounds SAHA (**1**) and **9** were evaluated against three human cancer cell lines, human non-small cell lung carcinoma A549 cells, human colorectal HCT116 cells, and human prostate cancer PC3 cells (Table 1). Among all the synthetic molecules, compound **10** showed the highest antiproliferative activity. Although the IC_{50} values of compounds **10** and **1** against HeLa cellular HDAC are comparable, **10** displayed 6- to 42-fold more potent antiproliferative activity than compound **1**, suppressing the growth of A549, HCT116, and PC3 cells with IC_{50} values of 72.52, 43.91, and 33.09 nM, respectively. Compound **11**, which has negligible anti-HDAC activity, showed 3- to 20-fold improvement of antiproliferative activity as compared with **1**. The retained cellular potency of compound **11** can probably be attributed to its inclusion of the structure of compound **9**. A similar phenomenon was observed with compound **12** which has better cellular activity but poorer anti-HDAC activity than compound **1**. The impact of central core structure (**9**, shown in bold) on antiproliferative activity was assessed by altering the pattern of substitution shown in compounds **15**–**17**. Removal of the 6-OMe group led to dramatic losses of cytotoxicity in compounds **15** and **16**, when compared with **10** and **13**, respectively. Replacement of the 3′,4′,5’-trimethoxybenzoyl group ring of antitubulin agents with 4’-methoxybenzoyl (**17**) also resulted in a loss of cellular activity. Despite all synthetic compounds have weaker antiproliferative activity than compound **9**, the core structure is essential for antiproliferative activity and it causes HDAC inhibitors to suppress the

growth of cancer cells at submicromolar IC_{50} levels.

2.2.3. In vitro tubulin polymerization assay

The effect of compounds **1**, **10**, and **12**–**17** on the assembly of tubulin is shown in Fig. 3. To confirm their influence on microtubule dynamics, paclitaxel, a tubulin stabilizer, and vincristine, a tubulin assembly inhibitor, were selected as reference compounds in the assay. The results indicate that compounds **12**–**14** dose-dependently inhibit the polymerization of tubulin remarkably and this explains the inconsistency of the anti-HDAC activity with the antiproliferative activity of compounds **12** and **14** (Table 1). Aside from HDAC inhibitory activity, compounds **12** and **14** may suppress the growth of cancer cells by inhibiting the polymerization of tubulin. In addition, the loss of cellular activity after altering the substitution pattern of the core structure (**15** vs **10**, **16** vs **11**, and **17** vs **12**) may be attributed to the disappearance of tubulin depolymerization activity. In summary, this series of 3-aroylindole hydroxamic acids could possibly serve as potent anticancer agents with dual tubulin and HDAC inhibitory activity.

2.2.4. HDAC isoform inhibition

Table 2 shows the selective inhibitory activity of the tested compounds (**10**–**13** and **15**–**17**) and the reference compound (**1**, SAHA) against HDAC1, 2, and 6. When compared with other isoenzymes, compound **15** tends to suppress the activity of HDAC1. It inhibits HDAC1 with an IC_{50} value of 138.76 nM, and is thus 16.7- and 5.7-fold more selective over HDAC2 and 6, respectively. The profile of compound **13** is similar to that of compound **1**. Notably, compound **12** with the same 4-(*N*-hydroxyaminocarbonyl)benzyl moiety as compound **5** shows highly selective activity on HDAC6 with selectivity ratios of 8, 21, and 14 over HDAC1, 2, and 8, respectively. Comparison of **10** and **15** reveals that the removal of the 6-OMe group possibly contributes to a slight enhancement of HDAC1 and HDAC2 inhibitory activity, as well as a slight decrease against HDAC6. This result is also seen in the comparison of **12** with **17**. The conversion of the 3′,4′,5’-trimethoxybenzoyl motif (**12**) into 4’-methoxybenzoyl one (**17**) led to the loss of HDAC6 selectivity over that of HDAC1 or HDAC2.

2.2.5. Western Blot analysis

The influence of compounds **10**, **12**, **13**, **15**, **16**, **17**, and the reference compound **1** on the expression of α-tubulin and histone H3 were assessed by the Western Blot analysis shown in Fig. 4. The results indicated that all tested compounds, with the exception of **10** and **15**, are able to increase the acetylation level of α-tubulin and histone H3 in dose-dependent manner, behavior comparable to that of compound **1**. Compound **10** showed a slight effect on the acetylation of α-tubulin, and compound **15** had negligible impact on the acetylation of histone H3. The expression of MPM2 (mitotic protein monoclonal-2) bands shows the cell cycle progression after treatment with tested compounds. The distinct bands appearing after treatment with compounds **10** and **12** indicated these two compounds probably cause cell cycle arrest at the M-phase, and this can be attributed to the tubulin polymerization inhibition of the compounds. Compounds **15**–**17** showed slight to negligible expression of MPM2 bands, which is consistent with the results shown in Fig. 3.

2.2.6. Growth inhibition of human prostate cancer xenografts in vivo

Compound **12** was further tested for its in vivo efficacy using a PC3 xenograft nude mouse model (Fig. 5A). Once a tumor was approximately 150 mm^3 in size after subcutaneous injection with 1×10^7 PC3 cells per mouse, the mice were randomized into vehicle control and treatment groups, with control mice receiving only the vehicle (1.0% carboxymethyl cellulose + 0.5% Tween80 in D5W). The result indicated that oral administration of compound **12** at doses of 100 and 200 mg/kg led to the suppression of PC3 cancer cell xenografts by $p < 0.01$ and factors of 24.8% and 68.5% (percent tumor growth inhibition [%TGI] values), respectively. In addition, the treatment with different doses of compound **12** had no significant effect on the body weight of tested mice (Fig. 5B).

2.2.7. Growth inhibition of multiple myeloma RPMI-8226 xenografts in vivo

Recently, the use of LBH589 in combination with bortezomib and dexamethasone has been approved by US FDA in 2015 for the treatment of multiple myeloma [8,9]. In addition, the combination therapy using ACY1215, an HDAC6 inhibitor, with bortezomib is currently undergoing clinical trials for treatment of multiple myeloma [22]. As a result, compound **12** was also tested for its ability to inhibit the growth of multiple myeloma xenografts in vivo, using bortezomib (Velcade®) (1 mg/kg, ip, once a week) as a reference compound. The result showed that compound **12** dose-dependently suppressed the growth of multiple myeloma (Fig. 6A). The intraperitoneal administration of compound **12** at doses of 50 and 100 mg/kg daily led to the suppression of RPMI-8226 cancer cell xenografts by TGI values of 35.8% ($p < 0.05$) and 58.2% ($P < 0.01$) (percent tumor growth inhibition [%TGI] values), respectively. It is noteworthy that compound **12** did not influence the change of weight of test animals, whereas the treatment with bortezomib caused three deaths of test animals (Fig. 6B).

3. Conclusion

The modification of compound **9** with various hydroxamic acid-containing groups provided a series of 3-aroylindole hydroxamic acids (**10**–**17**). Five of the eight compounds showed HDAC enzymatic activity comparable to that of compound **1**. An in vitro antiproliferation assay showed that the presence of the core structure (**9**) plays a crucial role in the cytotoxicity regardless of the HDAC enzymatic potency. In addition to the HDAC inhibitory activity, compounds **10** and **12**–**14** also possess tubulin depolymerization ability. Compound **12** displayed 8-fold selectivity for HDAC6 over HDAC1 and 21-fold over HDAC2, and suppressed the growth of tumors in human prostate PC3 xenograft models with a $p < 0.01$ by TGI factors of 24.8% and 68.5% after oral administration with 100 and 200 mg/kg, respectively. The intraperitoneal administration of compound **12** at doses of 50 and 100 mg/kg also suppresses RPMI-8226 cancer cell xenografts by TGI of 35.8% and 58.2%, respectively. Taken together, the combination of compound **9** with hydroxamic acid-containing moieties results in a series of novel 3-aroylindoles as antitumor molecules with safer profiles.

4. Experimental section

4.1. Chemistry

Nuclear magnetic resonance (^1H and ^{13}C NMR) spectra were recorded with a Bruker DRX-500 spectrometer (operating at 500 MHz) or a Bruker Fourier 300 (operating at 300 MHz), with chemical shifts in parts per million (δ) downfield from TMS, the internal standard. High-resolution mass spectra (HRMS) were recorded with a JEOL (JMS-700) electron impact (EI) mass spectrometer. The purities of the final compounds were determined using an Agilent 1100 series HPLC system using a C-18 column (Agilent ZORBAX Eclipse XDB-C18 5 μm, 4.6 mm × 150 mm) and were found to be ≥ 95%. Flash column chromatography was conducted using silica gel (Merck Kieselgel 60, No. 9385, 230–400 mesh ASTM). All reactions were conducted under an atmosphere of dry N_2.

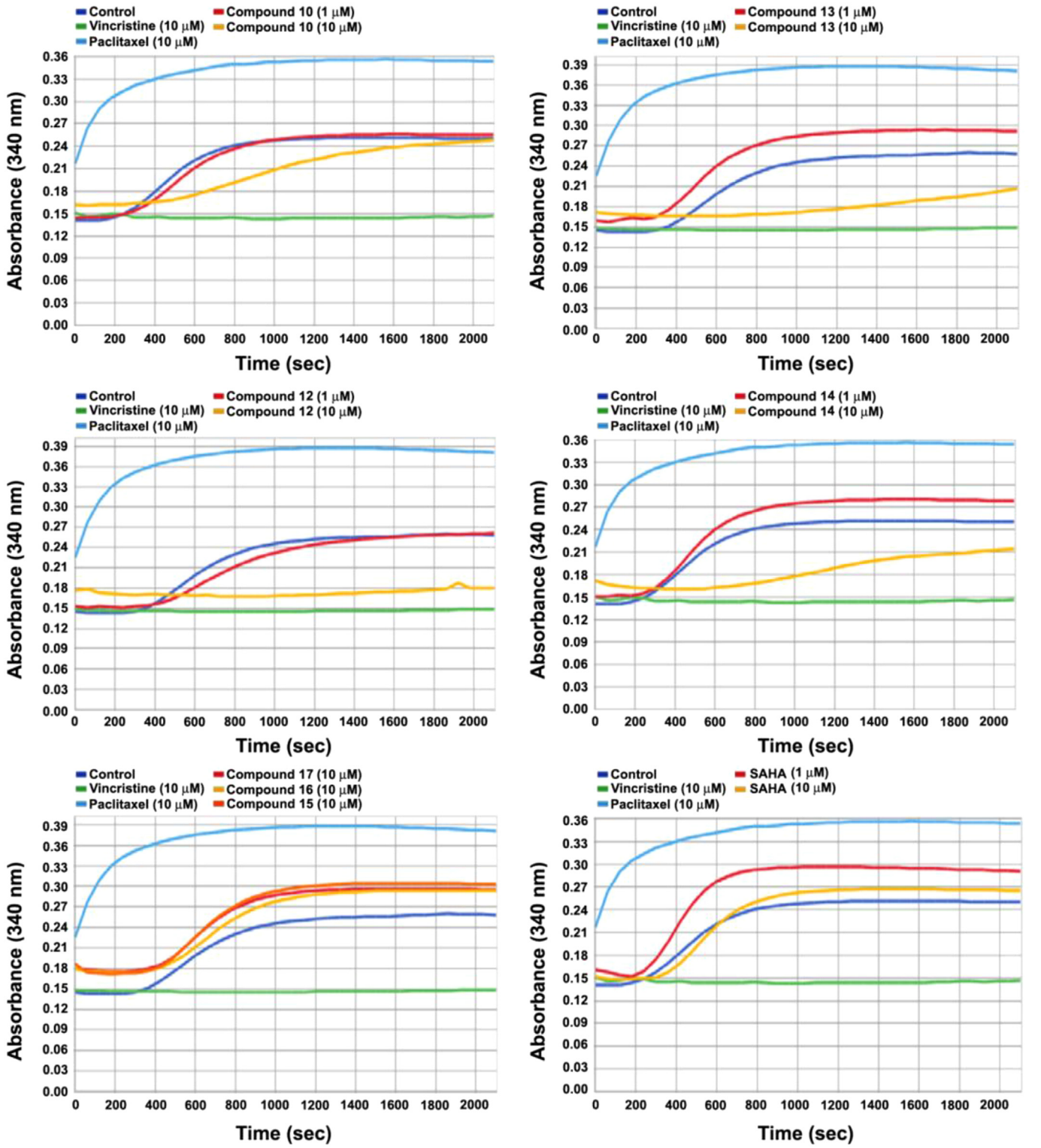

Fig. 3. *In vitro* tubulin polymerization assay. Microtubule assembly was assessed using the CytoDYNAMIX Screen kit BK006P, (Cytoskeleton Inc., Denver, CO). Purified porcine tubulin proteins (>99% purity) were suspended in G-PEM buffer containing 80 mM PIPES, 2 mM $MgCl_2$, 0.5 mM EGTA, 1 mM GTP (pH 6.9), and 15% glycerol in the absence or presence of indicated compounds at 4 °C. The mixture was immediately transferred to pre-warmed 96-well plates, and absorbance was measured at 340 nm every 1 min for 30 min using a 37 °C plate reader (SpectraMAX Plus, Molecular Devices Inc., Sunnyvale, CA).

*4.1.1. (E)-N-Hydroxy-3-(3-(6-methoxy-3-(3,4,5-trimethoxybenzoyl)-1H-indol-1-ylsulfonyl)phenyl)- acrylamide (**10**)*

A mixture of compound **22** (0.5 g, 0.82 mmol) and trifluoroacetic acid (10 mL) was stirred at room temperature for 16 h. The reaction was quenched with H_2O and extracted with EtOAc (25 mL × 3). The organic layer was extracted with saturated aqueous $NaHCO_3$ (50 mL × 2). The combined organic layer was dried over anhydrous $MgSO_4$ and concentrated under reduced pressure to give a brown residue which was purified by silica gel chromatography (EtOAc/n-hexane = 1:2) to give the acrylic acid product. The resulting product

Table 2
HDAC inhibition activity and isoform selectivity of tested compounds.

Compd	IC_{50} (nM)[a]			selectivity ratio	
	HDAC1	HDAC2	HDAC6	HDAC1/HDAC6	HDAC2/HDAC6
10	467.82 ± 7.80	3215.90 ± 31.73	275.35 ± 14.47	1.7	11.68
11	>10,000	>10,000	>10,000	–	–
12	573.43 ± 40.21	1408.14 ± 63.24	64.50 ± 2.44	8.89	21.83
13	129.57 ± 8.48	287.59 ± 4.37	70.49 ± 5.64	1.84	4.08
15	138.76 ± 19.46	2319.76 ± 87.21	791.60 ± 48.78	0.18	2.93
16	141.12 ± 4.57	385.51 ± 18.98	138.13 ± 3.88	1.02	2.79
17	157.62 ± 10.17	209.35 ± 3.15	108.48 ± 5.84	1.45	1.93
1	101.98 ± 8.73	332.65 ± 15.52	72.34 ± 1.89	1.41	4.60

[a] SD: standard deviation. All experiments were independently performed at least three times.

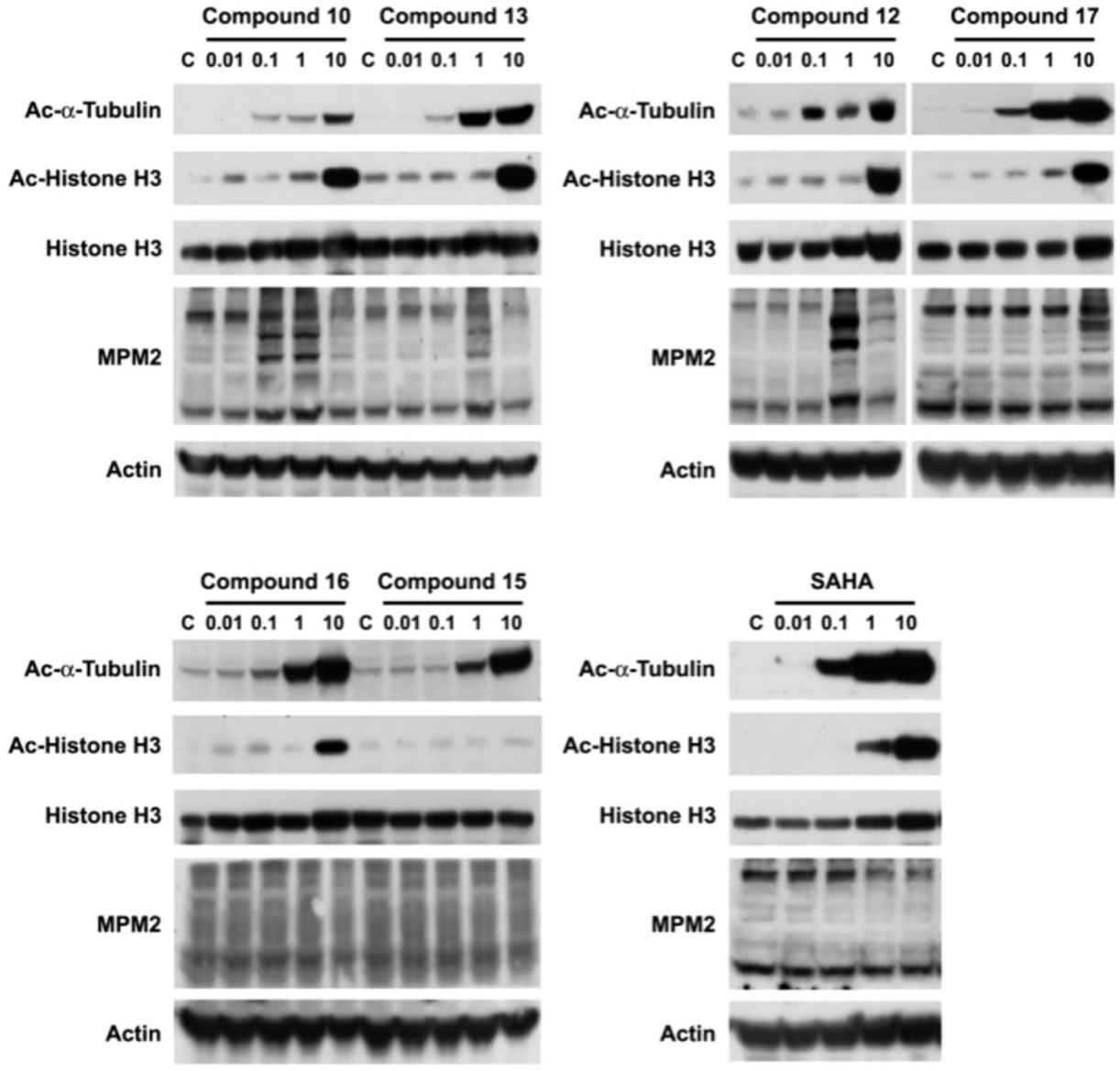

Fig. 4. Effect of α-tubulin acetylation and histone H3 acetylation in cultured human prostate PC3 cells by compounds **10**, **12**, **13**, **15**, **16**, **17**, and **1** using Western blot analysis.

(0.3 g, 0.54 mmol) was dissolved in DMF (4 mL), then EDC·HCl (0.16 g, 0.81 mmol), HOBt (0.09 g, 0.65 mmol), NMM (0.15 mL, 1.23 mmol), and NH_2OTP (0.08 g, 0.64 mmol) were added and the mixture was stirred at room temperature for 2 h. The reaction was quenched with water and extracted with EtOAc (100 mL × 3). The organic layer was dried over anhydrous $MgSO_4$ and concentrated under reduced pressure. The resulting residue was purified by flash column chromatography (CH_2Cl_2/CH_3OH/aqueous NH_3 = 20:1:1) to give a white solid. To the resulting product was added 10% trifluoroacetic acid in MeOH (10 mL) and the mixture was stirred at room temperature for 16 h. The reaction was quenched with H_2O and extracted with EtOAc (25 mL × 3). The organic layer was

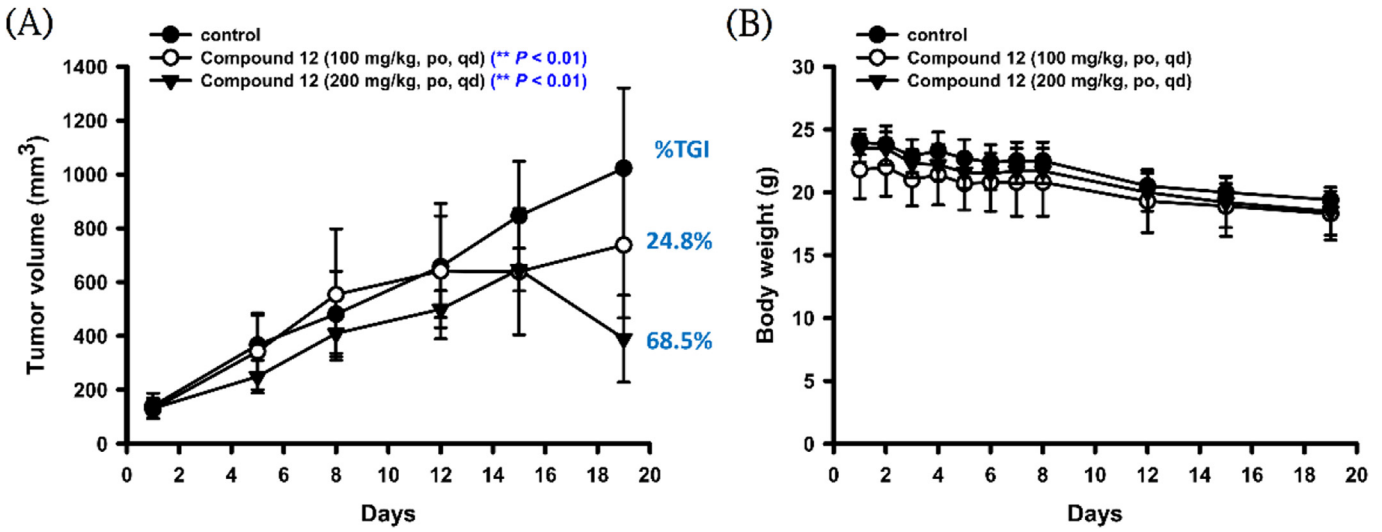

Fig. 5. (A) Anticancer activity of compound **12** in a xenograft model of human prostate PC3 cells. Tumor growth of PC3 xenograft nude mice treated with or without compound **12** (100 and 200 mg/kg) was tracked by the mean tumor volume (mm^3) ± S.E and calculated as % tumor growth inhibition (%TGI). Tumor volume was determined using caliper measurements and was calculated as the product of 1/2 × length × $width^2$. (B) Body weight (g) of the mice. *, $p < 0.05$, **$p < 0.01$, and ***$p < 0.001$ as compared with the control group.

extracted with saturated aqueous $NaHCO_3$ (50 mL × 2). The combined organic layer was dried over anhydrous $MgSO_4$ and concentrated under reduced pressure to give a brown residue which was purified by column chromatography (EtOAc: n-hexane = 1: 2) to afford compound **10** (43%). mp 151–152 °C; ^{1}H NMR (300 MHz, Acetone-d_6) δ 10.51 (s, 1H), 8.10–8.24 (m, 3H), 7.98 (d, J = 7.8 Hz, 1H), 7.70 (d, J = 7.8 Hz, 1H), 7.58–7.64 (m, 2H), 7.23 (s, 2H), 7.08 (dd, J = 2.1, 8.7 Hz, 1H), 6.72 (d, J = 15.6 Hz, 1H), 3.96 (s, 9H), 3.88 (s, 3H). HRMS (ESI) for $C_{28}H_{26}N_2O_9S$ ($M + H^+$) calcd 566.1359, found 566.1436. HPLC purity of 94.10% (retention time = 34.48).

4.1.2. (E)-N-Hydroxy-3-(4-(6-methoxy-3-(3,4,5-trimethoxybenzoyl)-1H-indol-1-ylsulfonyl)phenyl)- acrylamide (**11**)

This compound was obtained from in 55% overall yield compound **20** in a manner similar to that described for the preparation of **10** from **19**: mp 225–226 °C; ^{1}H NMR (500 MHz, Acetone-d_6) δ 8.22–8.26 (m, 3H), 8.13 (d, J = 9.0 Hz, 1H), 7.96 (d, J = 8.4 Hz, 2H), 7.69 (d, J = 16.2 Hz, 1H), 7.63 (d, J = 2.1 Hz, 1H), 7.24 (s, 2H), 7.10 (dd, J = 2.4, 9.0 Hz, 1H), 7.69 (d, J = 16.2 Hz, 1H), 3.97 (s, 9H), 3.89 (s, 3H). HRMS (ESI) for $C_{28}H_{26}N_2O_9S$ (M^+) calcd 566.1359, found: 566.1407. HPLC purity of 97.33% (retention time = 35.93).

4.1.3. N-Hydroxy-4-((6-methoxy-3-(3,4,5-trimethoxybenzoyl)-1H-indol-1-yl)methyl)benzamide (**12**)

A mixture of compound **26** (1.0 g, 2.04 mmol) dissolved in MeOH (20 mL), and 1 N LiOH (5 mL) was heated under reflux for 3 h. To the reaction was added H_2O (50 mL) followed by acidification with 3 N HCl and extraction with EtOAc (50 mL × 3). The organic layers were collected and purified by column chromatography to afford a white solid (0.87 g). The resulting product (0.6 g, 1.26 mmol) was dissolved in DMF (4 mL), and EDC·HCl (0.32 g, 1.62 mmol), HOBt (0.18 g, 1.3 mmol), NMM (0.15 mL, 1.23 mmol) and NH_2OTP (0.16 g, 1.28 mmol) were added. After stirring at room temperature for 2 h, the reaction was quenched with H_2O and extracted with EtOAc (50 mL × 3). The combined organic layer was dried over anhydrous $MgSO_4$ and concentrated under reduced pressure. The residue was purified by silica gel chromatography (CH_2Cl_2/CH_3OH/aqueous NH_3 = 20:1:1) to give a white solid. To the solid was added 10% TFA in MeOH (10 mL) and the mixture was stirred at room temperature for 16 h. The reaction mixture was quenched with H_2O and extracted with EtOAc (25 mL × 3), and then the organic layer was washed with saturated aqueous $NaHCO_3$ (50 mL × 2). The combined organic layers were dried over anhydrous $MgSO_4$ and concentrated under reduced pressure to give a brown residue, which was purified by silica gel chromatography (EtOAc/n-hexane = 1:2) to give compound **12** (66%). mp 181–182 °C; ^{1}H NMR (300 MHz, acetone-d_6) δ 8.27 (d, J = 9.0 Hz, 1H), 8.06 (s, 1H), 7.82 (d, J = 8.4 Hz, 2H), 7.45 (d, J = 8.4 Hz, 2H), 7.15 (s, 2H), 7.10 (d, J = 2.1 Hz, 1H), 6.96 (dd, J = 2.1, 8.7 Hz, 1H), 5.64 (s, 2H), 3.89 (s, 6H), 3.82 (s, 6H). HRMS (ESI) for $C_{27}H_{26}N_2O_7$ (M^+) calcd 490.1740, found 490.1817. HPLC purity of 95.00% (retention time = 25.21).

4.1.4. (E)-N-Hydroxy-3-(4-((6-methoxy-3-(3,4,5-trimethoxybenzoyl)-1H-indol-1-yl)methyl)-phenyl)- acrylamide (13)

This compound was obtained in 55% overall yield from compound **28** in a manner similar to that described for the preparation of **10** from **19**: mp 186–187 °C; ^{1}H NMR (300 MHz, acetone-d_6) δ 8.28 (d, J = 8.4 Hz, 1H), 8.05 (s, 1H), 7.50–7.63 (m, 3H), 7.41 (d, J = 8.4 Hz, 2H), 7.13–7.20 (m, 3H), 6.97 (dd, 2.4, 8.7 Hz, 1H), 5.60 (s, 2H), 3.90 (s, 6H), 3.85 (s, 3H), 3.83 (s, 3H). HRMS (ESI) for $C_{29}H_{28}N_2O_7$ (M^+) calcd 516.1897, found: 516.1962. HPLC purity of 98.06% (retention time = 26.67).

4.1.5. N-(2-Amino-phenyl)-4-[6-methoxy-3-(3,4,5-trimethoxy-benzoyl)-indol-1-ylmethyl]-benzamide (14)

Compound **26** (1.0 g, 2.04 mmol) was dissolved in MeOH (20 mL), 1 N LiOH (5 mL) was added and the mixture was heated under reflux for 3 h. To the reaction was added H_2O (50 mL) and this was followed by acidification with 3 N HCl and extraction with EtOAc (50 mL × 3). The organic layers were collected and purified by column chromatography to afford a white solid (0.87 g). The resulting product (0.4 g, 0.8 mmol) was dissolved in DMF (4 mL), and HOBt (0.2 g, 1.5 mmol), EDC·HCl (0.17 g, 0.8 mmol), NMM (0.25 mL), and *o*-phenylenediamine (0.12 g, 1.1 mmol) were added. After stirring at room temperature for 2 h, H_2O (30 mL) was added to the reaction mixture and the resulting brown precipitate was collected by filtration and purified by column chromatography (*n*-

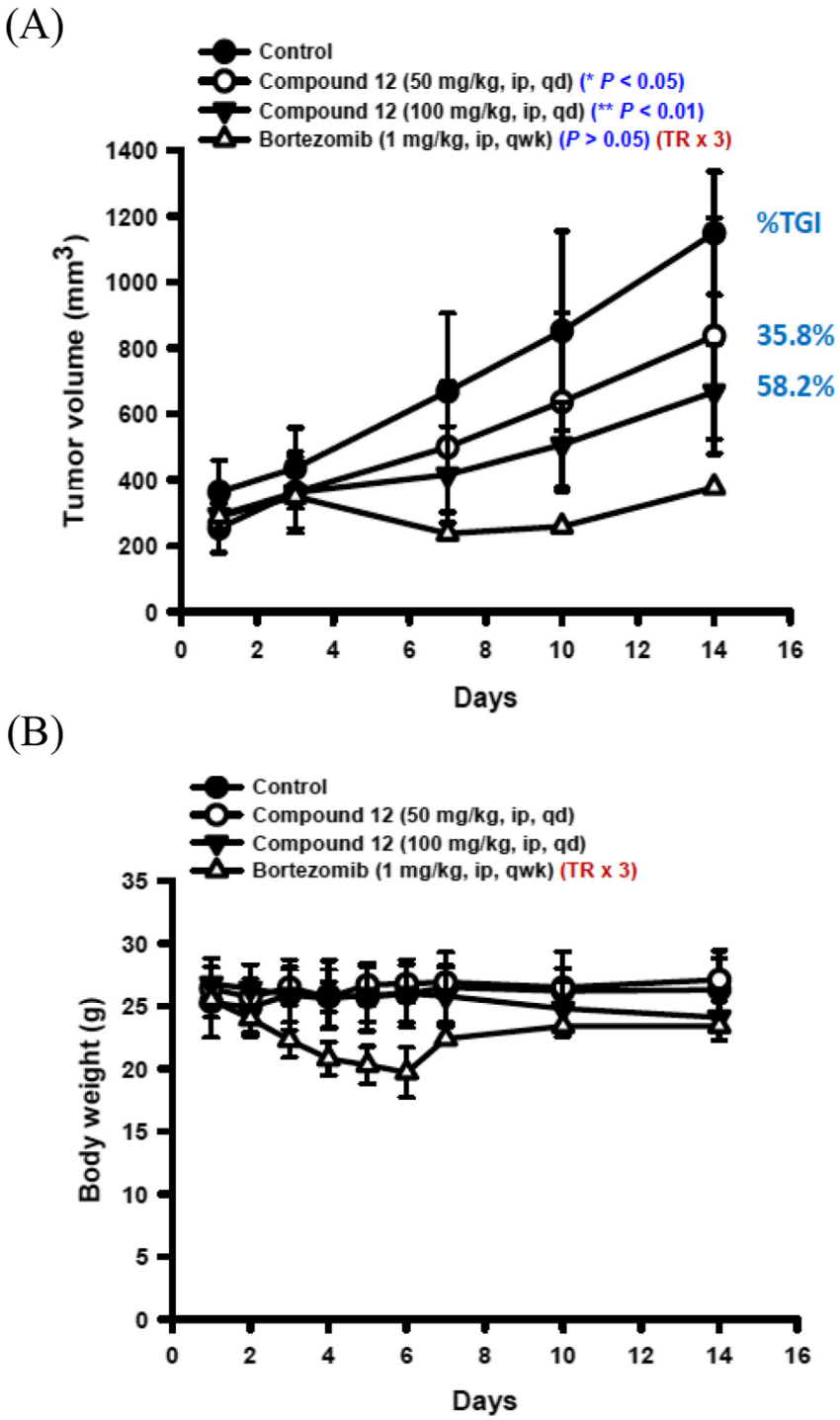

Fig. 6. (A) Anticancer activity of compound **12** in a xenograft model of multiple myeloma RPMI-8226 cells. Tumor growth of RPMI-822 xenograft nude mice treated with or without compound **12** (50 and 100 mg/kg) was tracked by the mean tumor volume (mm^3) ± S.E and calculated as % tumor growth inhibition (%TGI). Tumor volume was determined using caliper measurements and was calculated as the product of 1/2 × length × $width^2$. (B) Body weight (g) of the mice. *, $p < 0.05$, **$p < 0.01$, and ***$p < 0.001$ as compared with the control group. TR: treatment-related death.

hexane/EtOAc = 1:4) to afford compound **14** (70%) as a brown solid. mp 150–151 °C; ^{1}H NMR (300 MHz, DMSO-d_6) δ 9.58 (s, 1H), 8.25 (s, 1H), 8.12 (d, J = 8.7 Hz, 1H), 7.91 (s, J = 8.1 Hz, 2H), 7.46 (d, J = 8.1 Hz, 2H), 7.08–7.15 (m, 4H), 6.89–6.98 (m, 2H), 6.75 (d, J = 7.2 Hz, 1H), 6.56 (t, J = 7.8 Hz, 1H), 5.59 (s, 2H), 3.86 (s, 6H), 3.79 (s, 3H), 3.76 (s, 3H). HRMS (ESI) for $C_{33}H_{31}N_3O_6$ (M^+) calcd 565.2213, found 565.2264. HPLC purity of 99.20% (retention time = 34.75).

4.1.6. (E)-N-Hydroxy-3-(3-(3-(3,4,5-trimethoxybenzoyl)-1H-indol-1-ylsulfonyl)phenyl)-acrylamide (15)

This compound was obtained in 40% overall yield from compound **21** in a manner similar to that described for the preparation of **10** from **19**: mp 172–173 °C; ^{1}H NMR (300 MHz, DMSO-d_6) δ 8.40 (s, 2H), 8.13–8.19 (m, 2H), 8.08 (d, J = 8.1 Hz, 2H), 7.94 (d, J = 7.8 Hz, 1H), 7.65 (t, J = 7.8 Hz, 1H), 7.4–7.53 (m, 3H), 7.19 (s, 2H), 6.57 (d,

J = 15.9 Hz, 2H), 3.86 (s, 6H), 3.80 (s, 3H). HRMS (ESI) for $C_{27}H_{24}N_2O_8S$ (M^+) calcd 536.1253, found 536.1332. HPLC purity of 100.0% (retention time = 33.24).

4.1.7. N-Hydroxy-4-[3-(3,4,5-trimethoxy-benzoyl)-indol-1-ylmethyl]-benzamide (16)

This compound was obtained in 48% overall yield from compound **29** in a manner similar to that described for the preparation of **10** from **19**: ^{1}H NMR (500 MHz, acetone-d_6) δ 10.35 (s, 1H), 8.37–8.41 (m, 1H), 8.18 (s, 1H), 7.51–7.58 (m, 4H), 7.37 (d, J = 7.5 Hz, 2H), 7.27–7.30 (m, 2H), 7.14 (s, 2H), 6.53 (d, J = 16.0 Hz, 1H), 5.63 (s, 2H), 3.88 (s, 6H), 3.80 (s, 3H). HRMS (ESI) for $C_{28}H_{27}N_2O_6$ ($M+H^+$) calcd 487.1869, found: 487.1858. HPLC purity of 98.23% (retention time = 30.04).

4.1.8. N-Hydroxy-4-((6-methoxy-3-(4-methoxybenzoyl)-1H-indol-1-yl)methyl)benzamide (17)

This compound was obtained in 65% overall yield from compound **25** in a manner similar to that described for the preparation of **12** from **9**: mp 120–121 °C; ^{1}H NMR (300 MHz, acetone-d_6) δ 8.26 (d, J = 8.4 Hz, 1H), 7.99 (s, 1H), 7.87–7.92 (m, 2H), 7.81 (d, J = 8.4 Hz, 2H), 7.39 (d, J = 8.4 Hz, 2H), 7.04–7.08 (m, 3H), 6.94 (dd, J = 2.4, 8.7 Hz, 1H), 5.64 (s, 2H), 3.91 (s, 3H), 3.80 (s, 3H). MS (EI): m/z (%):431.1602 (100); HRMS (ESI) for $C_{25}H_{22}N_2O_5$ (M^+) calcd 430.1602, found 430.1529. HPLC purity of 97.11% (retention time = 30.45).

4.1.9. [1-(3-Bromo-benzenesulfonyl)-6-methoxy-1H-indol-3-yl]-(3,4,5-trimethoxy-phenyl)- methanone (19)

3-Bromobenzenesulfonyl chloride (4.12 g, 16.11 mmol) was added to a mixture of **9** (5.0 g, 10.65 mmol) and 60% of NaH (0.64 g, 16.11 mmol) in anhydrous DMF (50 mL) and the mixture was stirred at room temperature for 3 h. The reaction was quenched with H_2O, and extracted with EtOAc (100 mL × 3). The combined organic layer was dried over anhydrous $MgSO_4$ and dried *in vacuo* to give a yellow residue which was purified by flash column chromatography (*n*-hexane: EtOAc = 4: 1) to afford compound **19** as a white powder. ^{1}H NMR (300 MHz, $CDCl_3$) δ 8.13 (d, J = 9.0 Hz, 1H), 8.06 (s, 1H), 7.90 (s, 1H), 7.84 (d, J = 9.0 Hz, 1H), 7.73 (d, J = 9.0 Hz, 1H), 7.50 (d, J = 0.9 Hz, 1H), 7.39 (t, J = 9.0 Hz, 1H), 7.13 (s, 2H), 7.02–7.05 (m, 1H), 3.92–3.97 (m, 12H).

4.1.10. [1-(4-Bromo-benzenesulfonyl)-6-methoxy-1H-indol-3-yl]-(3,4,5-trimethoxy-phenyl)- methanone (20)

This compound was obtained yield from compound **9** in a manner similar to that described for the preparation of **19**: ^{1}H NMR (500 MHz, $CDCl_3$) δ 8.11 (d, J = 10.0 Hz, 1H), 7.89 (s, 1H), 7.75 (dd, J = 1.5, 7.0 Hz, 2H), 7.61 (dd, J = 1.5, 7.0 Hz, 2H), 7.49 (d, J = 2.5 Hz, 1H), 7.12 (s, 2H), 7.02 (dd, J = 2.5, 8.5 Hz, 1H), 3.96 (s, 3H), 3.91 (s, 6H), 3. 93 (s, 3H).

4.1.11. (1-(3-Bromophenylsulfonyl)-1H-indol-3-yl)(3,4,5-trimethoxyphenyl)methanone (21)

This compound was obtained from compound **18** in a manner similar to that described for the preparation of **19** from **9**: ^{1}H NMR (300 MHz, $CDCl_3$) δ 8.23–8.28 (m, 1H), 8.05 (t, J = 1.8 Hz, 1H), 7.80–8.02 (m, 2H), 7.85–7.89 (m, 1H), 7.70–7.74 (m, 1H), 7.33–7.47 (m, 3H), 7.13 (s, 2H), 3.97 (s, 3H), 3.92 (s, 6H).

4.1.12. (E)-tert-Butyl-3-(3-(6-methoxy-3-(3,4,5-trimethoxybenzoyl)-1H-indol-1-ylsulfonyl)) phenyl acrylate (22)

A mixture of compound **19** (6.7 g, 11.95 mmol), $Pd(OAc)_2$ (1.47 g, 6.58 mmol), PPh_3 (1.57 g, 5.98 mmol), K_2CO_3 (1.65 g, 11.95 mmol), triethylamine (1.7 mL, 11.95 mmol), *tert*-butyl acrylate (2.6 mL, 17.93 mmol), and anhydrous DMF (5 mL) was stirred at 100 °C for 5 h. The reaction mixture was cooled to ambient temperature and filtered through a pad of Celite. The filtrate was concentrated under reduced pressure and the resulting brown residue was purified by flash column chromatography (*n*-hexane: EtOAc = 2: 1) to afford compound **22** as a yellow oil. ^{1}H NMR (500 MHz, $CDCl_3$) δ 8.11 (d, J = 9.0 Hz, 1H), 8.02 (s, 1H), 7.93 (s, 1H), 7.86 (d, J = 8.0 Hz, 1H), 7.60–7.72 (m, 2H), 7.45–7.53 (m, 2H), 7.37 (d, J = 7.0 Hz, 1H), 7.13 (s, 2H), 7.02 (dd, J = 2.5, 9.0 Hz, 1H), 6.38 (d, J = 16.0 Hz, 1H), 3.97 (s, 3H), 3.92 (m, 9H), 1.33 (s, 9H).

4.1.13. 4-[6-Methoxy-3-(3,4,5-trimethoxy-benzoyl)-indol-1-ylmethyl]-benzoic acid methyl ester (26)

NaH (0.15 g, 3.8 mmol) was added to a solution of compound **9** (0.9 g, 2.6 mmol) in DMF (5 mL) and the mixture was stirred for 20 min. Methyl (4-chloromethyl)benzoate (0.52 g, 2.8 mmol) was added to the resulting mixture which was then stirred for 16 h. The reaction was quenched with H_2O (50 mL) and extracted with EtOAc (50 mL × 3). The organic layers were collected and dried in vacuum to afford compound **26** (1.19 g, 94%) as an oily product. ^{1}H NMR (500 MHz, $CDCl_3$) δ 7.94 (d, J = 8.5 Hz, 2H), 7.60 (d, J = 9.0 Hz, 1H), 7.19 (d, J = 8.0 Hz, 2H), 7.12–7.15 (m, 3H), 6.86 (dd, J = 2.0, 8.5 Hz, 1H), 6.68 (s, 1H), 5.83 (s, 2H), 5.29 (s, 1H), 3.93 (s, 3H), 3.89 (s, 6H), 3.87 (s, 3H), 3.81 (s, 3H).

4.1.14. (1-(4-Bromobenzyl)-6-methoxy-1H-indol-3-yl)(3,4,5-trimethoxyphenyl)methanone (28)

NaH (0.15 g, 3.8 mmol) was added to a solution of compound **9** (0.9 g, 2.6 mmol) in DMF (5 mL) and the mixture was stirred for 20 min. Methyl 4-bromobenzyl bromide (0.8 g, 3.2 mmol) was added to the resulting mixture which was then stirred for 16 h. The reaction was quenched with H_2O (50 mL) and extracted with EtOAc (50 mL × 3). The organic layers were collected and dried in vacuum to afford compound **28** as an oily product. ^{1}H NMR (300 MHz, $CDCl_3$) δ 8.27 (d, J = 6.0 Hz, 1H), 7.40–7.51 (m, 3H), 6.97–7.10 (m, 5H), 6.74 (d, J = 3.0 Hz, 1H), 5.25 (s, 2H), 3.91 (s, 3H), 3.84 (s, 6H), 3.83 (s, 3H).

4.2. Biology

4.2.1. HeLa nuclear HDAC enzyme inhibition

The HeLa nuclear extract HDAC activity was measured by using the HDAC Fluorescent Activity Assay Kit (BioVision, CA) according to manufacturer's instructions. Briefly, the HDAC fluorometric substrate and assay buffer were added to HeLa nuclear extracts in a 96-well format and incubated at 37 °C for 30 min. The reaction was stopped by adding lysine developer, and the mixture was incubated for another 30 min at 37 °C. Additional negative controls included incubation without the nuclear extract, without the substrate, or without both. TSA at 1 μM was used as the positive control. A fluorescence plate reader with excitation at 355 nm and emission at 460 nm was used to quantify HDAC activity.

4.2.2. In vitro cell growth inhibitory activity

4.2.2.1. Cell culture. All human cancer cells were maintained in RPMI 1640 medium containing 100 units/mL penicillin G sodium, 100 μg/mL streptomycin sulfate, 0.25 μg/mL amphotericin B, and 25 μg/mL gentamicin. The medium was supplemented with 10% fetal bovine serum. The cells were cultured in a humidified incubator at 37 °C, in an atmosphere of 5% CO_2 and 95% air.

4.2.2.2. The sulforhodamine B (SRB) assay. Cell proliferation was determined with the SRB assay. Human cancer A549 (non-small cell lung cancer), HCT116 (human colon carcinoma), and PC-3 (prostate) cells were seeded in 96-well plates in medium with 5% FBS. Cells were fixed with 10% trichloroacetic acid (TCA) to

represent the cell population at the time of compound addition (T_0) after 24 h. Then additional incubation of DMSO or test compound for 48 h, cells were fixed with 10% TCA and SRB at 0.4% (w/v) in 1% acetic acid. Unbound SRB was washed out by 1% acetic acid and SRB bound cells were solubilized with 10 mM Trizma base to determine the absorbance at 515 nm. Using the following absorbance measurements, time zero (T_0), control growth (C), and cell growth in the presence of the compound (T_x), the percentage growth was calculated at each of the compound concentration levels. Growth inhibition of 50% (GI_{50}) was calculated from [(Ti-Tz)/(C-Tz)] x 100 = 50. GI_{50} (inhibition rate of cell proliferation) was calculated as the test drug concentration that reduced cell proliferation by 50%.

4.2.3. Western blot analysis

Human prostate cancer PC3 cells were harvested using a lysis buffer (2.5 mM sodium pyrophosphate, 1 mM EGTA, 1 mM EDTA, 150 mM NaCl, 1 mM PMSF, 1 mM Na_3VO_4, 1 mM NaF, 0.1% Triton X-100 in 20 mM Tris–HCl buffer, pH 7.5), and then centrifuged at 13,000 rpm for 30 min. Cell lysates were collected and analyzed by immunoblotting with specific antibodies. The signals were visualized using an enhanced chemiluminescence (ECL) detection system (Amersham, Buckinghamshire, UK).

4.2.4. HDAC enzymes inhibition assays

Fluorogenic HDAC assay kits (BPS Bioscience Corp., San Diego, CA, USA) were used to assess the ability of HDAC inhibitors to inhibit deacetylation of lysine residues on the substrate by recombinant HDAC1, 2, or 6, according to the manufacturer's instructions.

4.2.5. In vitro tubulin polymerization assay

Microtubule assembly was assessed using the CytoDYNAMIX Screen kit (BK006P, Cytoskeleton Inc., Denver, CO). Purified porcine tubulin proteins (>99% purity) were suspended in G-PEM buffer containing 80 mM PIPES, 2 mM $MgCl_2$, 0.5 mM EGTA, 1 mM GTP (pH 6.9), and 15% glycerol in the absence or presence of indicated compounds at 4 °C. The mixture was immediately transferred to pre-warmed 96-well plates, and absorbance was measured at 340 nm every 1 min for 30 min using a plate reader at 37 °C (SpectraMAX Plus, Molecular Devices Inc., Sunnyvale, CA).

4.2.6. Antitumor activity in vivo

Male nude athymic mice (male, 5–6 weeks) were subcutaneously injected with 1×10^7 prostate cancer PC3 cells and multiple myeloma RPMI-8226 cells per mouse. When tumor volumes reached approximately 150–350 mm^3, mice were randomized by tumor size as follows: In the prostate cancer PC3 xenograft model: vehicle (5% DMSO + 5% Cremophor in D5W), 100 mg/kg compound **12**, 200 mg/kg compound **12** by oral administration daily. In the multiple myeloma RPMI-8226 xenograft model: vehicle (5% DMSO + 5% Cremophor in D5W), 50 mg/kg compound **12**, 100 mg/kg compound **12** by intraperitoneal injection daily. Tumor volumes were calculated using caliper measurements twice per week using the formula volume (mm^3) = (length × $width^2$)/2. %TGI (Tumor Growth Inhibition) as determined by the formula: {1-[(T_t/T_0)/(C_t/C_0)]/1-[C_0/C_t]}*100. T_t: tumor volume of treated at time t. T_0: tumor volume of treated at time 0. C_t: tumor volume of control at time t. C_0: tumor volume of control at time 0. Body weights were measured daily during the first week and twice per week.

Acknowledgments

This research were supported by the National Science Council of the Republic of China (grant no. MOST 103-2113-M-038 -001 -MY3).

Appendix A. Supplementary data

Supplementary data related to this article can be found at http://dx.doi.org/10.1016/j.ejmech.2016.11.033.

References

[1] W. Guerrant, V. Patil, J.C. Canzoneri, A.K. Oyelere, Dual targeting of histone deacetylase and topoisomerase II with novel bifunctional inhibitors, J. Med. Chem. 55 (2012) 1465–1477.
[2] J.B. Chen, T.R. Chern, T.T. Wei, C.C. Chen, J.H. Lin, J.M. Fang, Design and synthesis of dual-action inhibitors targeting histone deacetylases and 3-hydroxy-3-methylglutaryl coenzyme A reductase for cancer treatment, J. Med. Chem. 56 (2013) 3645–3655.
[3] M. Duvic, R. Talpur, X. Ni, C. Zhang, P. Hazarika, C. Kelly, J.H. Chiao, J.F. Reilly, J.L. Ricker, V.M. Richon, S.R. Frankel, Phase 2 trial of oral vorinostat (suberoylanilide hydroxamic acid, SAHA) for refractory cutaneous T-cell lymphoma (CTCL), Blood 109 (2007) 31–39.
[4] I. Hoshino, H. Matsubara, N. Hanari, Histone deacetylase inhibitor FK228 activates tumor suppressor Prdx1 with apoptosis induction in esophageal cancer cells, Clin. Cancer Res. 11 (2005) 7945–7952.
[5] N. Noureen, H. Rashid, S. Kalsoom, Identification of type-specific anti-cancer histone deacetylase inhibitor: road to success, Cancer Chemother. Pharmacol. 66 (2010) 625–633.
[6] X. Qian, W.J. LaRochelle, G. Ara, F. Wu, K.D. Petersen, A. Thougaard, M. Sehested, H.S. Lichenstein, M. Jeffers, Activity of PXD101, a histone deacetylase inhibitor, in preclinical ovarian cancer studies, Mol. Cancer Ther. 5 (2006) 2086–2095.
[7] X. Qian, G. Ara, E. Mills, W.J. LaRochelle, H.S. Lichenstein, M. Jeffers, Activity of the histone deacetylase inhibitor belinostat (PXD101) in preclinical models of prostate cancer, Int. J. Cancer 122 (2008) 1400–1410.
[8] J.P. Laubach, P. Moreau, J.F. San-Miguel, P.G. Richardson, Panobinostat for the treatment of multiple myeloma, Clin. Cancer Res. 21 (2015) 4767–4773.
[9] K. Wahaib, A.E. Beggs, H. Campbell, L. Kodali, P.D. Ford, Panobinostat: a histone deacetylase inhibitor for the treatment of relapsed or refractory multiple myeloma, Am. J. Health. Syst. Pharm. 73 (2016) 441–450.
[10] B.I. Lee, S.H. Park, J.W. Kim, E.A. Sausville, H.T. Kim, O. Nakanishi, J.B. Trepel, S.J. Kim, MS-275, a histone deacetylase inhibitor, selectively induces transforming growth factor beta type II receptor expression in human breast cancer cells, Cancer Res. 61 (2001) 931–934.
[11] M.J. Lai, H.L. Huang, S.L. Pan, Y.M. Liu, C.Y. Peng, H.Y. Lee, T.K. Yeh, P.H. Huang, C.M. Teng, C.S. Chen, H.Y. Chuang, J.P. Liou, Synthesis and biological evaluation of 1-arylsulfonyl-5-(N-hydroxyacrylamide)indoles as potent histone deacetylase inhibitors with antitumor activity in vivo, J. Med. Chem. 55 (2012) 3777–3791.
[12] H.Y. Lee, A.C. Tsai, M.C. Chen, P.J. Shen, Y.C. Cheng, C.C. Kuo, S.L. Pan, Y.M. Liu, J.F. Liu, T.K. Yeh, J.C. Wang, C.Y. Chang, J.Y. Chang, J.P. Liou, Azaindolylsulfonamides, with a more selective inhibitory effect on histone deacetylase 6 activity, exhibit antitumor activity in colorectal cancer HCT116 cells, J. Med. Chem. 57 (2014) 4009–4022.
[13] S. Heerboth, K. Lapinska, N. Snyder, M. Leary, S. Rollinson, S. Sarkar, Use of epigenetic drugs in disease: an overview, Genet. Epigenet 6 (2014) 9–19.
[14] H. Rajak, A. Singh, K. Raghuwanshi, R. Kumar, P.K. Dewangan, R. Veerasamy, P.C. Sharma, A. Dixit, P. Mishra, A structural insight into hydroxamic acid based histone deacetylase inhibitors for the presence of anticancer activity, Curr. Med. Chem. 21 (2014) 2642–2664.
[15] H.P. Hsieh, J.P. Liou, N. Mahindroo, Pharmaceutical design of antimitotic agents based on combretastatins, Curr. Pharm. Des. 11 (2005) 1655–1677.
[16] X. Zhang, J. Zhang, L. Tong, Y. Luo, M. Su, Y. Zang, J. Li, W. Lu, Y. Chen, The discovery of colchicine-SAHA hybrids as a new class of antitumor agents, Bioorg. Med. Chem. 21 (2013) 3240–3244.
[17] X. Zhang, J. Zhang, M. Su, Y. Zhou, Y. Chen, J. Li, W. Lu, Design, synthesis and biological evaluation of 4'-demethyl-4-deoxypodophyllotoxin derivatives as novel tubulin and histone deacetylase dual inhibitors, RSC Adv. 4 (2014) 40444–40448.
[18] X. Zhang, Y. Kong, J. Zhang, M. Su, Y. Zhou, Y. Zang, J. Li, Y. Chen, Y. Fang, X. Zhang, W. Lu, Design, synthesis and biological evaluation of colchicine derivatives as novel tubulin and histone deacetylase dual inhibitors, Eur. J. Med. Chem. 95 (2015) 127–135.
[19] J.P. Liou, N. Mahindroo, C.W. Chang, F.M. Guo, S.W. Lee, U.K. Tan, T.K. Yeh, C.C. Kuo, Y.W. Chang, P.H. Lu, Y.S. Tung, K.T. Lin, J.Y. Chang, H.P. Hsieh, Structure-activity relationship studies of 3-aroylindoles as potent antimitotic agents, Chem. Med. Chem. 1 (2006) 1106–1118.
[20] J.P. Liou, Y.L. Chang, F.M. Kuo, C.W. Chang, H.Y. Tseng, C.C. Wang, Y.N. Yang, J.Y. Chang, S.J. Lee, H.P. Hsieh, Concise synthesis and structure-activity relationships of combretastatin A-4 analogues, 1-aroylindoles and 3-aroylindoles, as novel classes of potent antitubulin agents, J. Med. Chem. 47 (2004) 4247–4257.
[21] C.C. Kuo, H.P. Hsieh, W.Y. Pan, C.P. Chen, J.P. Liou, S.J. Lee, Y.L. Chang, L.T. Chen, C.T. Chen, J.Y. Chang, BPR0L075, a novel synthetic indole compound with antimitotic activity in human cancer cells, exerts effective antitumoral activity in vivo, Cancer Res. 64 (2004) 4621–4628.
[22] https://clinicaltrials.gov/ct2/home.